Sound fields near building facades – comparison of finite and semi-infinite reflectors on a rigid ground plane

C. Hopkins[1#] and Y. Lam[2]
[1]Acoustics Research Unit, School of Architecture, University of Liverpool, Liverpool L69 7ZN, UK
[2]Acoustics Research Centre, School of Computing, Science and Engineering, University of Salford, Salford M5 4WT, UK

[#]Corresponding author. Email: carl.hopkins@liv.ac.uk

Abstract

The sound field in front of, and close to a building facade is relevant to the measurement and prediction of environmental noise and sound insulation. For simplicity it is often assumed that the facade can be treated as a semi-infinite reflector, however in the low-frequency range (50 – 200 Hz) this is no longer appropriate as the wavelengths are similar or larger than the facade dimensions. Scale model measurements and predictions using Integral Equation Methods have been used to investigate the effect of diffraction on the sound field in front of finite size reflectors. For the situation that is commonly encountered in front of building facades, the results indicate that diffraction effects are only likely to be significant in the low-frequency range (50 – 200 Hz) when the façade dimensions are less than 5 m. This assumes that there is a point source close to the ground and microphones at a height of 1.2 or 1.5 m, at a distance between 1 and 2 m in front of the façade.

Keywords: façade, reflection, diffraction, integral equation methods, environmental noise, sound insulation

1. Introduction

To assess environmental noise in the built environment or sound transmission into a building it is necessary to measure or predict the external sound pressure level near a building facade. External microphone positions are often prescribed in measurement Standards to be at a distance of 1 or 2 m from the facade, and 1.2 to 1.5 m above the ground (e.g. see references 1–3).

To assess the effect of a facade on the measured sound pressure level the simplest approach is to assume that the facade can be treated as a semi-infinite reflector. The sound field in front of the facade can therefore be determined from the combination of the direct path from the source to the receiver, and the reflected paths that involve specular reflection from the ground and/or the facade. Real facades have a finite size but diffraction effects from the edges of the facade are expected to be negligible for microphone positions near the centre of the facade when the wavelength of sound is small compared to the facade dimensions. In practice it is often the low-frequency range (defined here as 50 – 200 Hz) that is of particular interest and in this range the wavelengths can be similar or larger than the facade dimensions.

Previous work by Hothersall & Simpson [2] produced a model to correct for the effect of the façade on a receiver position near the façade surface. This used a line source representing road traffic and assumed that the façade acted as a sufficiently large reflector that only geometrical reflection needed to be considered as with a semi-infinite reflector. Field measurements from Hall *et al* [3] with road traffic noise showed that for a microphone at a distance of 2 m from the façade, the assumption of energy doubling due to the presence of a façade was only reasonable above 200 Hz. Below 200 Hz there were significant differences and diffraction effects were noted as one possible cause. Experimental investigations on real facades by Quirt [4] looked at microphone positions on the surface of a façade and at a distance of 2 m from the façade. The results indicated that diffraction fringes were not dominant at measurement positions near corners of a building façade and that the main variations were due to interference effects from the ground surface. Previous work on diffraction and scattering

for source and receiver positions in front of finite reflectors has looked at their role as scattering objects or diffusers where the purpose was to alter the acoustics of performance spaces or studios (e.g. see Rindel [5], Cox and Lam [6]). Recently, Davy [7] has investigated the effect of diffraction with a finite reflector when the receiver position is on the surface of the reflector; this is relevant to facade sound insulation measurements that use surface microphones. Diffraction effects with small reflectors are also relevant to the measurement procedure used for the Calculation of Road Traffic Noise, CRTN [8]. This is because the procedure allows a temporary screen with an area of at least 1 m^2 to be positioned 1 m behind the microphone to act as a facade. Diffraction effects from a flat reflecting facade with a raised point source above the facade to simulate aircraft traffic have previously been measured using a scale model in the laboratory [9]. These measurements were in an anechoic space so no account was taken of reflections from the ground plane. In this paper the ground plane is included and the focus is on noise sources near the ground.

The effect of diffraction is awkward to assess with measurements near real buildings because of a large number of uncontrollable variables in the external environment, such as weather conditions and variable ground impedance. In addition real facades are formed from a wide variety of surfaces, some of which are profiled. To avoid these complications, this investigation into diffraction considered the sound field in front of a thin, flat, finite sized, rigid reflector representing a building facade. In practice a facade forms the surface of a three-dimensional building. The edge lengths for the building facade, such as side walls, roof, and other protrusions, can vary from a few tens of centimetres to several metres. This introduced too many additional variables for this study and the extension to consider diffraction effects with three-dimensional objects that form facades is left for future work.

In contrast to finite reflectors that are used to alter the room acoustics of performance spaces, there is rarely any need to accurately predict the diffraction effects for an individual facade. At frequencies below 200 Hz and at positions near the centre of the facade it is reasonable to assume that by modelling the facade as a thin plate it will be possible to gain an indication of when diffraction effects become significant for real building facades. This is assessed by using predictions for a semi-infinite reflector, predictions for different finite reflectors using Integral Equation Methods, and scale model measurements on finite size reflectors in the laboratory with a point source. Five square, flat, reflectors were considered that represented full-size facades with side dimensions of 2, 3, 4, 5 and 6 m. The source-receiver-reflector geometry used in the investigation is shown in Fig. 1. This geometry is essentially based around a road traffic scenario with buildings along the roadside for which the horizontal source-reflector distance of 14.5 m is similar to a reference distance used by Delany *et al* [10] for the prediction of road traffic noise. A point source was assumed to be at a height of 0.5 m above the ground; note that this height is commonly assumed for a line source used to represent a road traffic source. The receiver position was 1.2 m above the ground; this height is commonly used for microphones in external noise measurements near facades. The reflector-receiver distance, *d*, was varied between 0.1 and 2 m. In practice it seems reasonable to assume that receiver positions will not usually be near the edge of a façade, but near the centre of a facade. For this reason the receiver position in the measurements was offset from the vertical centre-line of the reflector by one-twelfth of the square reflector dimension.

2. Sound field in front of a semi-infinite reflector

For a semi-infinite reflector the sound field generated by a point source in front of the reflector can be calculated by considering the image sources shown in Fig. 2. The sound travels from the source (S) to the receiver (R) via four different paths: the first path is the direct path from the source to the receiver, the second path involves a single reflection from the ground, the third path involves a single reflection from the ground and a single reflection from the façade, and the fourth path involves a single reflection from the façade. The path lengths in terms of the distance, *d*, from the source, or image source, to the receiver are also indicated in the diagram.

It is assumed that: (a) there is a point source emitting spherical waves, (b) the ground and façade are perfectly reflecting with no phase change upon reflection, (c) all reflections are specular, (d) the façade has dimensions that are very large compared to the wavelength (i.e. a semi-infinite plate), and (e) there

are no other facades nearby that significantly affect the sound field. The assumption of specular reflection is reasonable for this situation, particularly below 1000 Hz; from Ismail and Oldham [11] it can generally be assumed that real facades have small scattering coefficients.

For many environmental noise and sound transmission calculations it is the free-field level that is needed, i.e. the level in the absence of the façade. For this reason it is convenient to look at the difference between the sound pressure level in front of the façade, and the free-field level without the façade. This requires the ratio of the total mean-square sound pressure, $\left\langle p^2 \right\rangle_t$, to the mean-square sound pressure, $\left\langle \left(p_1 + p_2 \right)^2 \right\rangle_t$; the latter term corresponds to the combination of the direct path between source and receiver (path length d_1), and the path in which the sound is reflected from the ground to the receiver (path length d_2). Hence the change in sound pressure level due to the presence of a reflector at single frequencies is

$$\frac{\left\langle p^2 \right\rangle_t}{\left\langle \left(p_1 + p_2 \right)^2 \right\rangle_t} = \frac{\left| \frac{\exp\left(-ikd_1\right)}{d_1} + \frac{\exp\left(-ikd_2\right)}{d_2} + \frac{\exp\left(-ikd_3\right)}{d_3} + \frac{\exp\left(-ikd_4\right)}{d_4} \right|^2}{\left| \frac{\exp\left(-ikd_1\right)}{d_1} + \frac{\exp\left(-ikd_2\right)}{d_2} \right|^2} \qquad \textbf{(1)}$$

where k is the wavenumber, and $\left\langle \ \right\rangle_t$ indicates the time-average value.

Destructive interference occurs where the path length difference, Δd_{pq}, between paths p and q, corresponds to a phase difference of an odd number of π radians,

$$2\pi \frac{\Delta d_{pq}}{\lambda} = \left(2n+1\right)\pi \qquad \textbf{(2)}$$

where n=0,1,2,3 etc.

Note that there are several path length differences for each value of n, but there will not be a dip in the spectrum that is calculated from Eqn. **1** at each of these interference frequencies because the spectrum is formed from the ratio of the combination of all four paths to the combination of two paths.

In many situations it is frequency bands and wide band noise signals that are of interest, for which the numerator and denominator of Eqn. **1** need to be rewritten; hence in the presence of the reflector the mean square pressure at the receiver is

$$\begin{aligned} \left\langle p^2 \right\rangle_t = \left\langle \left(p_1 + p_2 + p_3 + p_4 \right)^2 \right\rangle_t = \left\langle p_1^2 \right\rangle_t + \left\langle p_2^2 \right\rangle_t + \left\langle p_3^2 \right\rangle_t + \left\langle p_4^2 \right\rangle_t + 2\left\langle p_1 p_2 \right\rangle_t \\ +2\left\langle p_1 p_3 \right\rangle_t + 2\left\langle p_1 p_4 \right\rangle_t + 2\left\langle p_2 p_3 \right\rangle_t + 2\left\langle p_2 p_4 \right\rangle_t + 2\left\langle p_3 p_4 \right\rangle_t \end{aligned} \qquad \textbf{(3)}$$

and in the absence of the reflector, the mean square pressure at the receiver is

$$\left\langle \left(p_1 + p_2 \right)^2 \right\rangle_t = \left\langle p_1^2 \right\rangle_t + \left\langle p_2^2 \right\rangle_t + 2\left\langle p_1 p_2 \right\rangle_t \qquad \textbf{(4)}$$

Each of the cross terms in Eqns **3** and **4** can be written in terms of an autocorrelation function, $R(\tau_{pq})$ for paths p and q, where

$$\left\langle p_p p_q \right\rangle_t = R\left(\tau_{pq}\right)\sqrt{\left\langle p_p^2 \right\rangle_t \left\langle p_q^2 \right\rangle_t} \qquad \textbf{(5)}$$

and

$$R\left(\tau_{pq}\right) = \frac{\left\langle p_p p_q \right\rangle_t}{\sqrt{\left\langle p_p^2 \right\rangle_t \left\langle p_q^2 \right\rangle_t}} \qquad \textbf{(6)}$$

for a time delay, τ_{pq}, between paths p and q.

This autocorrelation function can now be found for a narrow band of noise where the lower and upper limits of the band (in terms of angular frequency) are ω_l and ω_u respectively. For a stationary random signal, $x(t)$, the spectral density, $S_x(\omega)$ is shown in Fig. 3 and the autocorrelation function, $R(\tau)$, is defined by

$$R\left(\tau\right) = \frac{E\left[x\left(t\right)x\left(t+\tau\right)\right]}{E\left[x^2\left(t\right)\right]} \qquad \textbf{(7)}$$

where $E[\ ]$ corresponds to the expected or mean value of the term within the square brackets. In Eqn. **7** these are

$$\begin{aligned} E\left[x\left(t\right)x\left(t+\tau\right)\right] &= \int_{-\infty}^{\infty} S_x\left(\omega\right)\exp\left(i\omega\tau\right)\mathrm{d}\omega = 2\int_{\omega_\mathrm{l}}^{\omega_\mathrm{u}} S_0 \cos\omega\tau\,\mathrm{d}\omega \\ &= \frac{4S_0}{\tau}\cos\left(\frac{\left(\omega_\mathrm{l}+\omega_\mathrm{u}\right)\tau}{2}\right)\sin\left(\frac{\left(\omega_\mathrm{u}-\omega_\mathrm{l}\right)\tau}{2}\right) \end{aligned} \qquad \textbf{(8)}$$

and

$$E\left[x^2\left(t\right)\right] = \int_{-\infty}^{\infty} S_x\left(\omega\right)\mathrm{d}\omega = 2S_0\left(\omega_\mathrm{u}-\omega_\mathrm{l}\right) \qquad \textbf{(9)}$$

which gives the autocorrelation function as

$$R\left(\tau\right) = \frac{2}{\left(\omega_\mathrm{u}-\omega_\mathrm{l}\right)\tau}\cos\left(\frac{\left(\omega_\mathrm{l}+\omega_\mathrm{u}\right)\tau}{2}\right)\sin\left(\frac{\left(\omega_\mathrm{u}-\omega_\mathrm{l}\right)\tau}{2}\right) \qquad \textbf{(10)}$$

Instead of a time delay, this autocorrelation function can now be written in terms of a path difference, Δd, in metres, using the relationship

$$\tau = \frac{\Delta d}{c_0} \qquad \textbf{(11)}$$

where c_0 is the speed of sound (m/s).

Hence for paths p and q, the autocorrelation function, $R(\Delta d_{pq})$ for each path length difference (magnitude), Δd_{pq}, is (Delany *et al* [12])

$$R\left(\Delta d_{pq}\right) = \frac{\lambda}{2\pi B \Delta d_{pq}} \cos\left(\frac{2\pi \Delta d_{pq}}{\lambda}\right) \sin\left(\frac{2\pi B \Delta d_{pq}}{\lambda}\right) \qquad \textbf{(12)}$$

where λ is the wavelength corresponding to the band centre frequency, i.e. $\lambda = 2c_0/(f_u + f_l)$, and $B = (f_u - f_l)/(f_u + f_l)$, which gives $B = 0.115$ for one-third-octave-bands, and $B = 0.332$ for octave-bands.

The pressures for the three indirect paths are related to the pressure for the direct path by taking account of geometrical spreading and the reflection coefficient (magnitude) for the ground, $\left|R_g\right|$, and for the façade acting as a reflector, $\left|R_f\right|$. Hence,

$$p_2 = \left|R_g\right| \frac{d_1}{d_2} p_1 \qquad p_3 = \left|R_g\right| \left|R_f\right| \frac{d_1}{d_3} p_1 \qquad p_4 = \left|R_f\right| \frac{d_1}{d_4} p_1 \qquad \textbf{(13)}$$

For a perfectly reflecting ground and façade, $\left|R_g\right| = \left|R_f\right| = 1$, and substituting Eqn. **13** into Eqns **3** and **4** gives the change in sound pressure level due to the presence of a reflector in frequency bands as

$$\frac{\left\langle p^2 \right\rangle_t}{\left\langle \left(p_1 + p_2\right)^2 \right\rangle_t} = \frac{\begin{array}{c} 1 + \left(\frac{d_1}{d_2}\right)^2 + \left(\frac{d_1}{d_3}\right)^2 + \left(\frac{d_1}{d_4}\right)^2 \\ + \frac{2d_1}{d_2} R\left(\Delta d_{12}\right) + \frac{2d_1}{d_3} R\left(\Delta d_{13}\right) + \frac{2d_1}{d_4} R\left(\Delta d_{14}\right) \\ + \frac{2d_1^2}{d_2 d_3} R\left(\Delta d_{23}\right) + \frac{2d_1^2}{d_2 d_4} R\left(\Delta d_{24}\right) + \frac{2d_1^2}{d_3 d_4} R\left(\Delta d_{34}\right) \end{array}}{1 + \left(\frac{d_1}{d_2}\right)^2 + \frac{2d_1}{d_2} R\left(\Delta d_{12}\right)} \qquad \textbf{(14)}$$

For the source-facade-receiver geometry in Fig. 1 and microphones that are 1 or 2 m from the façade, Fig. 4 shows the change in the sound pressure level due to the presence of a semi-infinite reflector that is calculated using Eqn. **14**. This indicates that there can be large fluctuations due to interference effects in the low-frequency range (50 – 200 Hz), but that in the mid-frequency range (250 – 1000 Hz), the assumption of energy doubling (3 dB) gives a reasonable estimate.

3. Predicting the sound field in front of finite reflectors using Integral Equation Methods

The Integral Equation Method (IEM) approach that is used for the numerical experiments is adapted for thin, rigid plates as described by Terai [13] (also see Kawai and Terai [14]). The software used for the calculations was the same as in the paper by Cox and Lam [6]. For comparison with the semi-

infinite plate model, the IEM calculations assumed that the source emitted spherical waves and that the ground and façade were perfectly reflecting with no phase change upon reflection. The radiating surface was divided into elements each representing a source radiating into the solid angle, 2π. Each element was represented by the value at its centre point and all element dimensions were $< \lambda/4$. By taking advantage of symmetry it was only necessary to define the element coordinates for half of the rigid plate, which reduced computation time.

The upper frequency was limited to 356 Hz for the 6 x 6 m reflector and 710 Hz for the 2 x 2 m reflector. This allowed coverage of the low-frequency range where it was expected that there would be large differences between finite and semi-infinite reflectors.

4. Scale model experiments

A 1:5 scale model was used for the measurements, but all the results and the accompanying discussion in this paper refer to dimensions and frequencies corresponding to the full-scale situation for a real facade.

The experiments were carried out in a semi-anechoic chamber with a concrete floor using a small loudspeaker as the sound source. The cut-off frequency of the chamber was approximately 250 Hz; which was below the lowest frequency of interest. The reflector was made from 30 mm thick, varnished board. A half-inch, free-field microphone was suspended in a string cradle to avoid scattering from the microphone stand. The signal processing was carried out with a PC-based MLSSA system which uses a Maximum Length Sequence (MLS) signal to give the impulse response. The frequency spectrum was then determined with an FFT frequency resolution of 3.66 Hz. Measurements were taken with and without the reflector to give the ratio given by the total mean-square sound pressure, p^2 , to the mean-square sound pressure, $(p_1+ p_2)^2$.

5. Results and discussion

For the smallest and largest reflectors (i.e. 2 x 2 m and 6 x 6 m), Fig. 5 to Fig. 8 show comparisons of measured and predicted changes in the sound pressure level due to the reflector for reflector-receiver distances of 0.1, 0.5, 1 and 2 m. Differences between the finite and semi-infinite reflectors are most noticeable at frequencies below 300 Hz. This is particularly apparent where the peaks and troughs occur at different frequencies and at different levels. The good agreement between the measurements and the IEM predictions provide evidence to support the observed differences between the finite and semi-infinite reflectors; an example of this can be seen in Fig. 6 where the 2 x 2 m reflector has a very shallow dip compared to the semi-infinite reflector at the lowest interference frequency. Note that differences in the depth of the *deep* interference dips (i.e. levels between -8 and -28 dB) are not always critical in this comparison; these partly depend on the frequency bandwidth or resolution that is chosen for the measurements and predictions. The upper frequency of interest is limited to 1000 Hz because at higher frequencies the turbulent air in the outdoor environment would usually reduce the coherence between the waves travelling along the different propagation paths [4,15]. As a result, the sharp minima in the spectrum due to destructive interference in outdoor measurements near real facades would be less likely to occur above 1000 Hz.

In practice, measurements are usually carried out in frequency bands which will smooth out some of the sharp interference patterns. Hence the measurements in one-third-octave-bands for the five reflectors with side dimensions of 2, 3, 4, 5 and 6 m are now compared with the prediction for the semi-infinite reflector. The intention is to assess the lowest frequency at which the finite reflectors can be considered as a semi-infinite reflector and to gain an indication of the significance of diffraction effects. Fig. 9 shows the difference between the measured finite reflectors and the predicted semi-infinite reflector for d=1 m and d=2 m. For d=1 m and reflector dimensions ≥4 m the difference can be considered as negligible at and above 125 Hz. For d=2 m and reflector dimensions ≥4 m the difference can be considered as negligible at and above 63 Hz. The fluctuations in these differences are specific to the source-reflector-receiver geometry. For this reason it is useful to assess the general trends using

measurements for a number of receiver-reflector distances in 0.1 m steps from 1 to 2 m inclusive as shown in Fig. 10. For the 4 x 4 m, 5 x 5 m and 6 x 6 m reflectors (Fig. 10a) the effects of diffraction are significant between the 63 and 100 Hz bands, but the effects can be considered as negligible above 100 Hz. Of particular interest is that the effects of diffraction are significant up to 250 Hz for the 3 x 3 m reflector (Fig. 10b), and up to 630 Hz for the 2 x 2 m reflector (Fig. 10c).

For frequency band measurements at a distance of 1 or 2 m from the facade, the combination of diffraction effects and interference effects in the low-frequency range (50 – 200 Hz) means that the assumption of energy-doubling will not always be valid. For a microphone at a distance of 2 m from housing façades this has previously been confirmed by field measurements with road traffic noise as the noise source [3].

Previous work on finite size reflectors has tended to focus on reflectors in concert halls to investigate limiting frequencies above which they can be treated as infinite reflectors. An early approach by Cremer was to consider a limiting frequency above which the reflector is effective in terms of specular reflection [16]. Later, Rindel [5,17] derived a frequency above which the attenuation due to diffraction is of minor importance. This used a Kirchoff-Fresnel approximation which assumed that the distances to the source and the receiver were large compared to the wavelength and the reflector dimensions. The extension to two-dimensional reflectors (e.g. a rectangular panel with edges in both x and y directions) was made by considering the diffraction effects in the two directions independently. This limiting frequency has been shown to give good estimates for single reflectors and an array of reflectors [6,17]. It is therefore of interest to compare Rindel's formula with the results in this paper.

From Rindel [5], the limiting frequency is

$$f_{\mathrm{L}} = \frac{c_0 d^*}{2S\cos\theta} \qquad \textbf{(15)}$$

where c_0 is the speed of sound, θ is the angle of incidence from the normal, S is the area of the reflector, and the distance d* is

$$d^* = \frac{2d_{\mathrm{r}}d_{\mathrm{s}}}{d_{\mathrm{r}} + d_{\mathrm{s}}} \qquad \textbf{(16)}$$

where d_{s} and d_{r} are the distances from the reflection point for the source and receiver respectively.

The assumptions that define this limiting frequency are not satisfied for the facade situation in this paper because: (a) the receiver distance is small compared to both the reflector dimensions and the wavelength at low-frequencies, and (b) it is not free-field (hence no account is taken of the combination of different paths). However it is still useful to assess whether it could give a reasonable estimate. For the geometry used in this paper the incident angle for each of the four paths is less than 8° so all the limiting frequencies can be calculated for normal incidence. Hence for the 2, 3, 4, 5 and 6 m square reflectors, the limiting frequencies are 151, 67, 38, 24, and 17 Hz for the receiver at 2 m from the facade, and 80, 36, 20, 13 and 9 Hz for the receiver at 1 m from the facade. These limiting frequencies are not good estimates of the frequency above which the effects of diffraction are negligible. For facades, it is therefore important to account for the effect of the short façade-receiver distance and ground reflection.

6. Conclusions

Good agreement between scale model measurements and predictions using Integral Equation Methods show that the effects of diffraction on the sound field in front of finite size reflectors can be significant

in the low-frequency range (50 – 200 Hz) and that both approaches are useful in quantifying the effect. For the situation commonly encountered in front of building facades, diffraction effects are only likely to be significant in the low-frequency range when façade dimensions are less than 5 m. This assumes that there is a point source close to the ground and the microphones are at a height of 1.2 or 1.5 m, and positioned at a distance between 1 and 2 m in front of the façade.

References

1. ISO 1996-1:1982. Description and measurement of environmental noise. Part 1: Guide to quantities and procedures. International Organization for Standardization.
2. Hothersall, DC and Simpson, S. The reflection of road traffic noise. Journal of Sound and Vibration 1983;90(3):399-405.
3. Hall, FL, Papakyriakou, MJ and Quirt, JD. Comparison of outdoor microphone locations for measuring sound insulation of building facades. Journal of Sound and Vibration 1984;92(4):559-567.
4. Quirt, JD. Sound fields near exterior building surfaces, Journal of the Acoustical Society of America 1985;77(2):557-566.
5. Rindel, JH. Design of new ceiling reflectors for improved ensemble in a concert hall, Applied Acoustics 1991;34:7-17.
6. Cox, TJ and Lam, YW. Evaluation of methods for predicting the scattering from simple rigid panels, Applied Acoustics 1993;40:123-140.
7. Davy, JL. A model for predicting diffraction on a finite flat surface as a function of angle of incidence and surface size, Internoise 2007, Istanbul, Turkey.
8. Anon. Calculation of road traffic noise. Department of Transport, Welsh Office. HMSO (London), 1988. ISBN 0115508473.
9. Bradley, JS and Chu, WT. Errors when using facade measurements of incident aircraft noise. Internoise 2002, USA.
10. Delany, ME, Harland, DG, Hood, RA and Scholes, WE. The prediction of noise levels L_{10} due to road traffic. Journal of Sound and Vibration 1976;48(3):305-325
11 . Ismail, MR and Oldham, DJ. A scale model investigation of sound reflection from building facades, Applied Acoustics 2005;66:123-147.
12. Delany, ME, Rennie, AJ and Collins, KM. Model evaluation of the noise shielding of aircraft ground-running pens, NPL Report Ac67 April 1974, National Physical Laboratory, UK.
13. Terai, T. On calculation of sound fields around three dimensional objects by Integral Equation Methods, Journal of Sound and Vibration 1980;69(1):71-100.
14. Kawai, Y and Terai, T. The application of Integral Equation Methods to the calculation of sound attenuation by barriers, Applied Acoustics 1990;31:101-117.
15. Attenborough, K. Review of ground effects on outdoor sound propagation from continuous broadband sources, Applied Acoustics 1988;24:289-319.
16. Cremer, L. Die Plexiglas-Reflektoren im neuen Herkulessaal der Münchner Residenz. Schalltechnik 1953;13(5):1-10.
17. Rindel, JH. Attenuation of sound reflections due to diffraction. Nordic Acoustical Meeting, Denmark 1986.

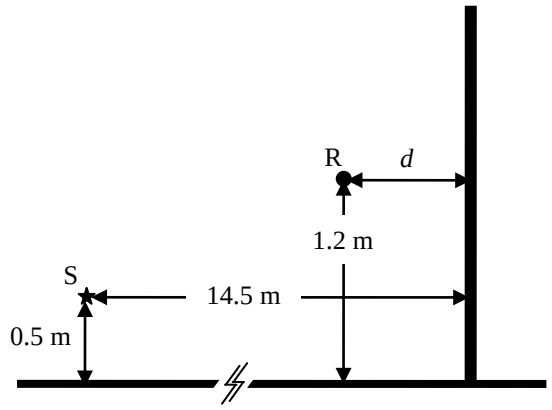

Fig. 1
Source-receiver-reflector geometry used for the comparison of measured and predicted data. These dimensions correspond to the full-scale situation for a real facade although a 1:5 scale model was used for the measurements.

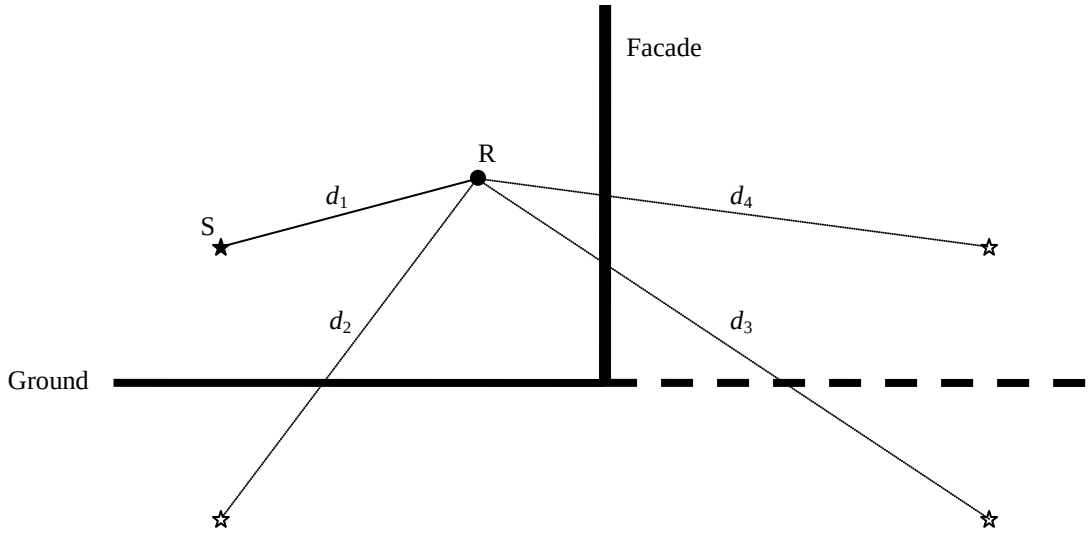

Fig. 2
Source (S) and receiver (R) orientation with image sources (☆) for the different propagation paths with path lengths, d_1, d_2, d_3 and d_4.

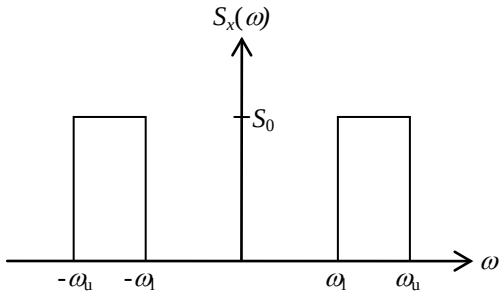

Fig. 3
Spectral density for a narrow band of noise.

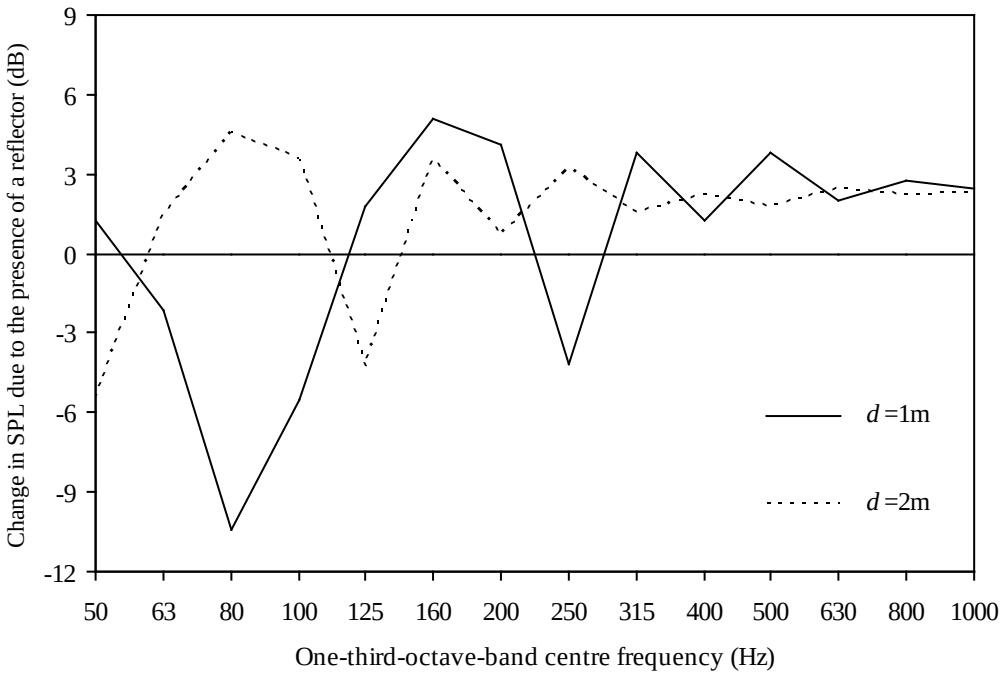

Fig. 4
Change in the sound pressure level due to the presence of a semi-infinite reflector for receiver positions that are at a distance of 1 m and 2 m from the façade (source and receiver positions given in Fig. 1).

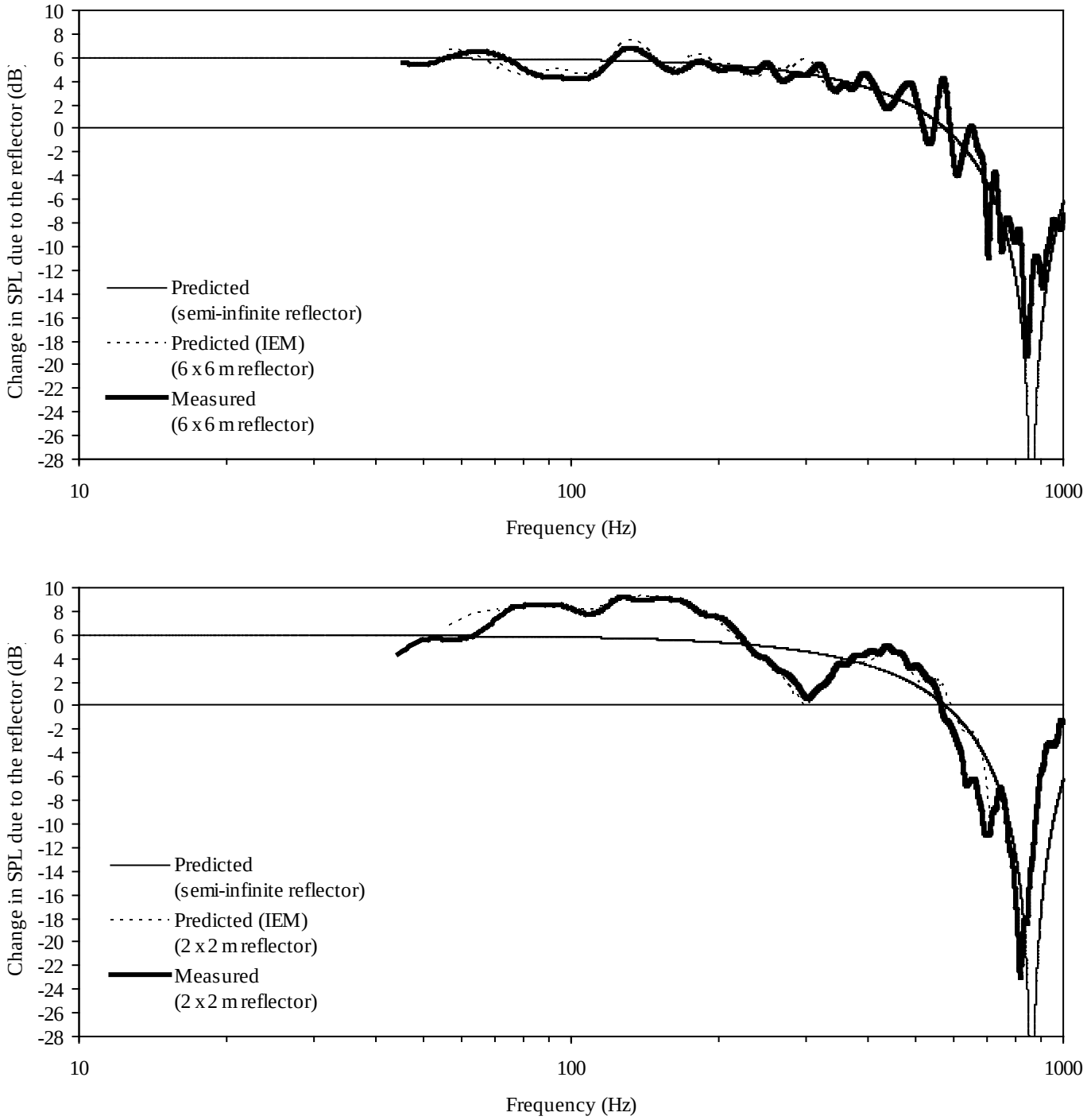

Fig. 5
Change in the sound pressure level due to the presence of the reflector: receiver-reflector distance, *d*=0.1 m.

Note to typesetter: Excel has cut off the closing bracket on the y-axis title. Please replace it.

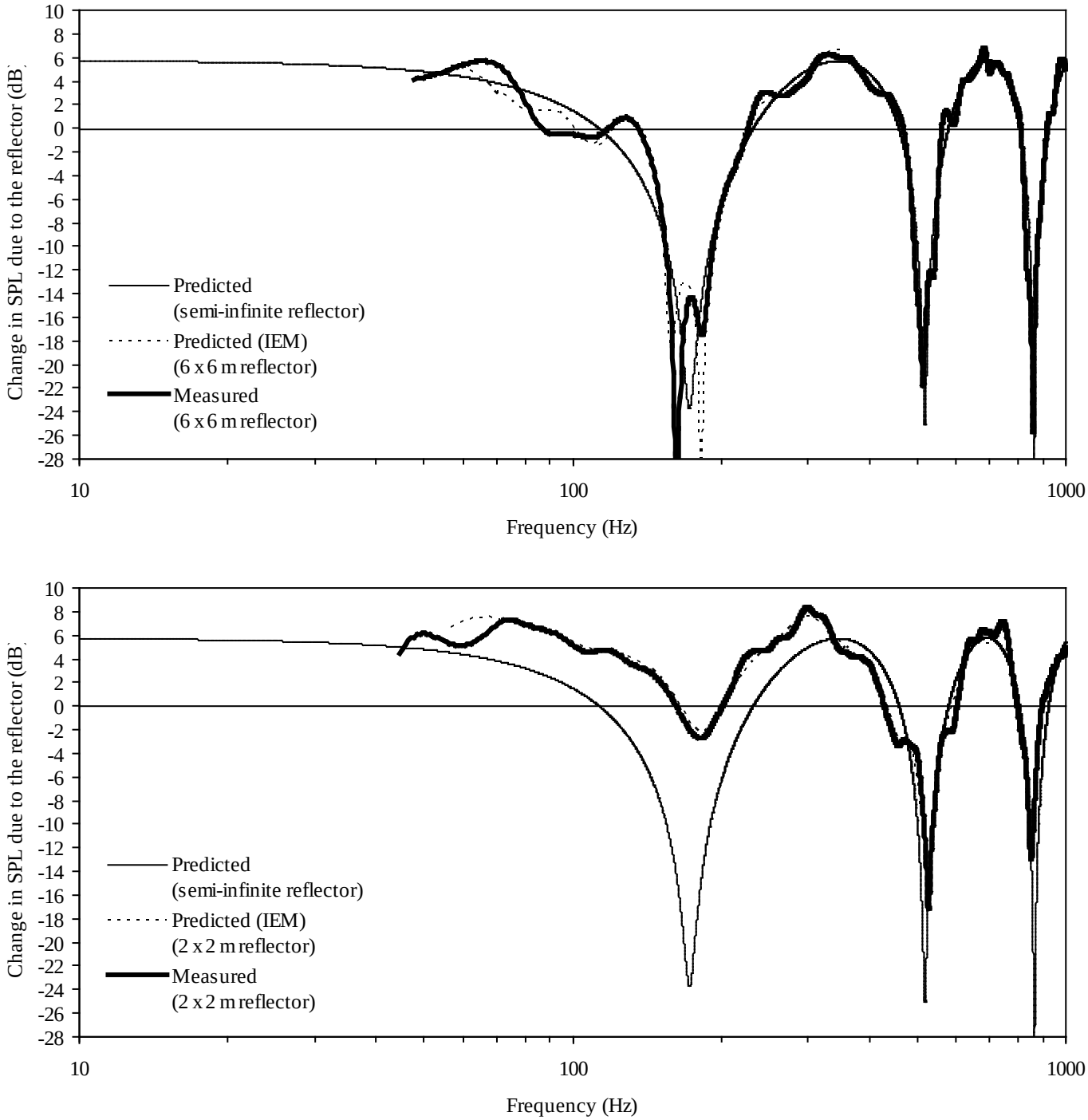

Fig. 6
Change in the sound pressure level due to the presence of the reflector: receiver-reflector distance, *d*=0.5 m.

Note to typesetter: Excel has cut off the closing bracket on the y-axis title. Please replace it.

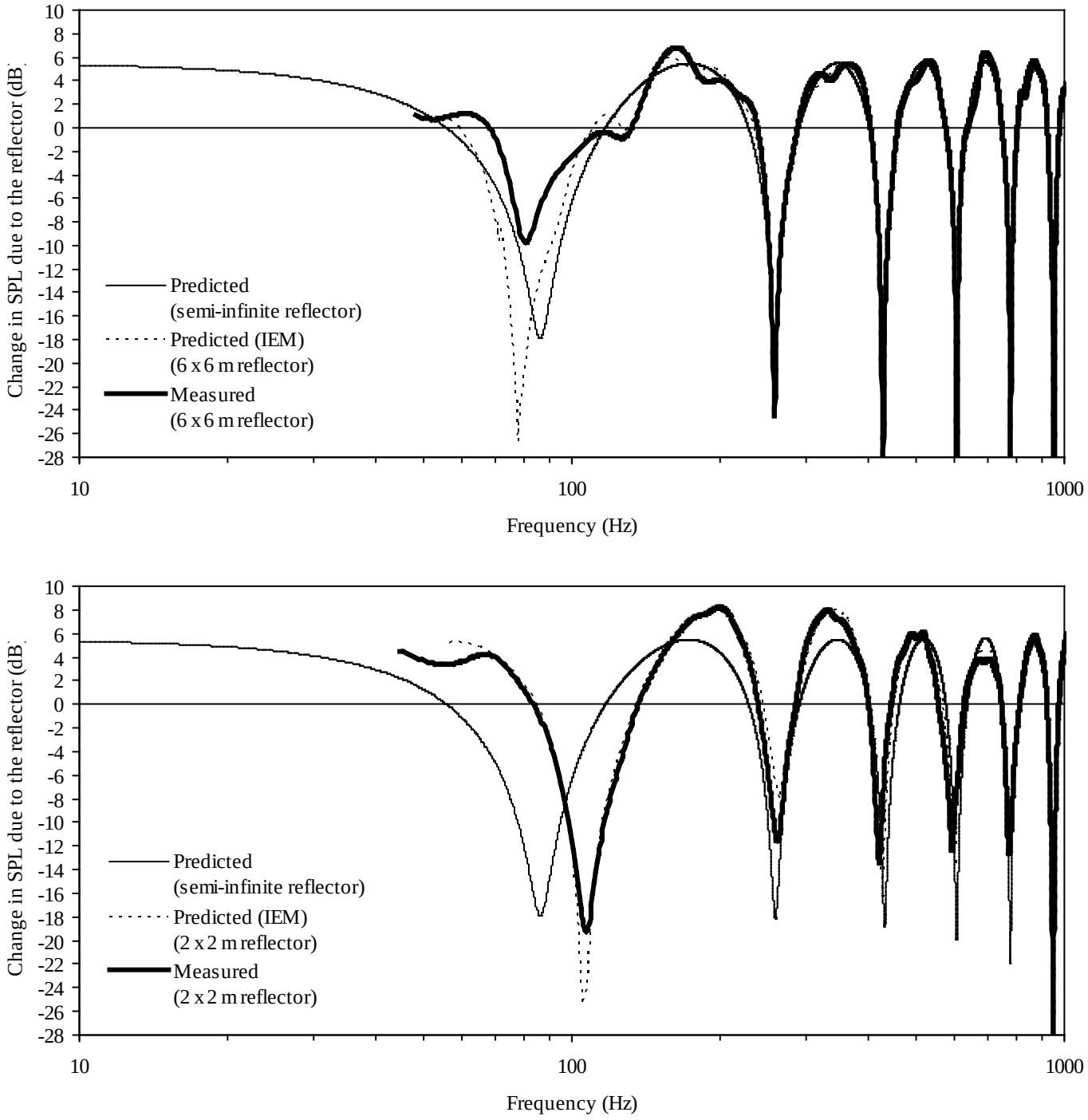

Fig. 7
Change in the sound pressure level due to the presence of the reflector: receiver-reflector distance, d=1.0 m.

Note to typesetter: Excel has cut off the closing bracket on the y-axis title. Please replace it.

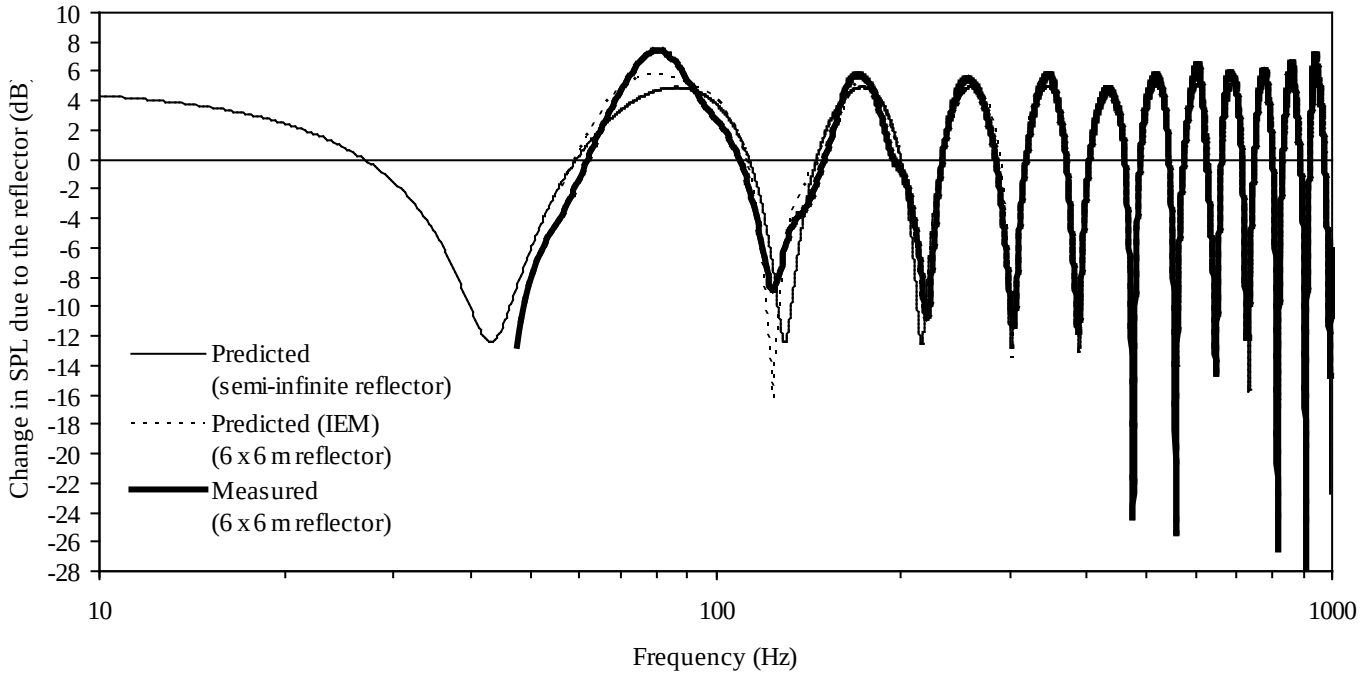

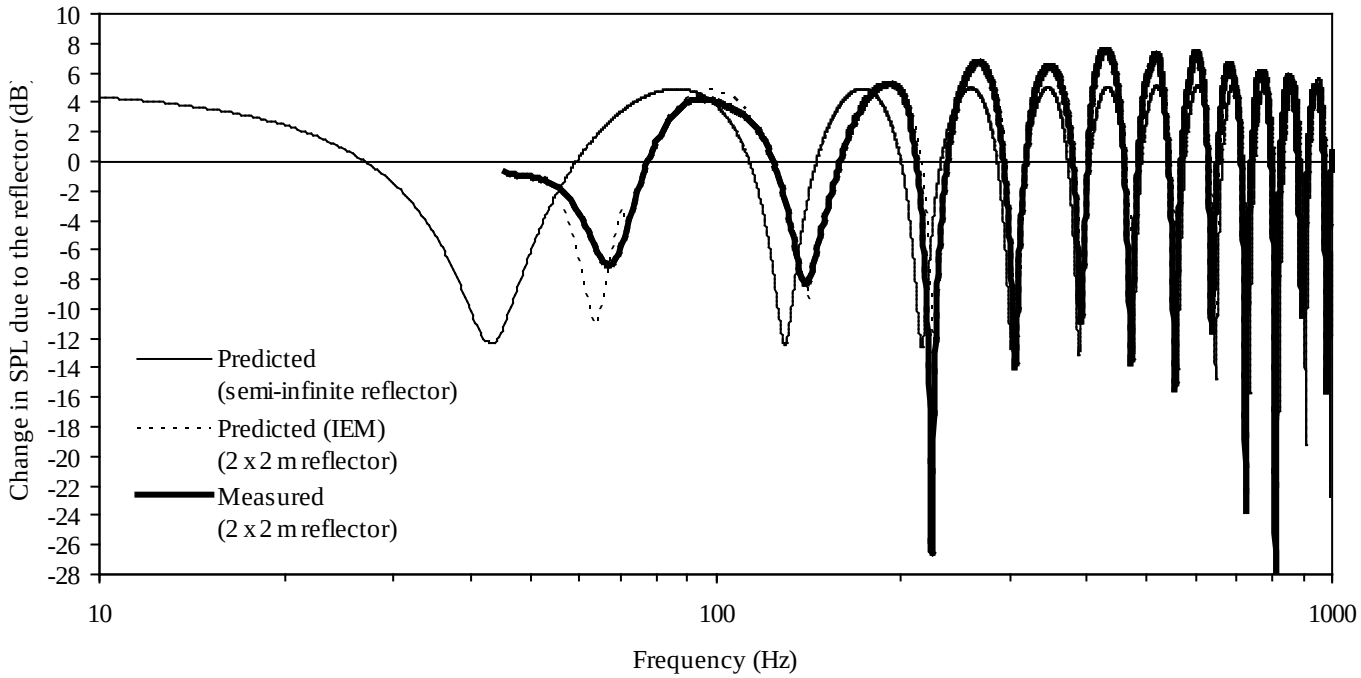

Fig. 8
Change in the sound pressure level due to the presence of the reflector: receiver-reflector distance, *d*=2.0 m.

Note to typesetter: Excel has cut off the closing bracket on the y-axis title. Please replace it.

a) *d*=1 m

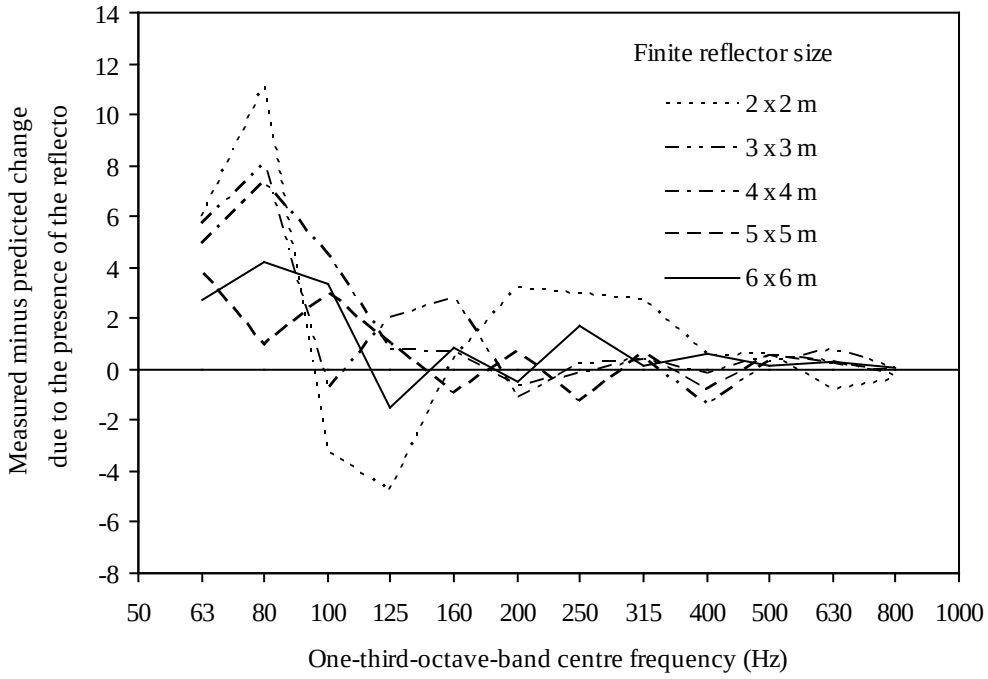

b) *d*=2 m

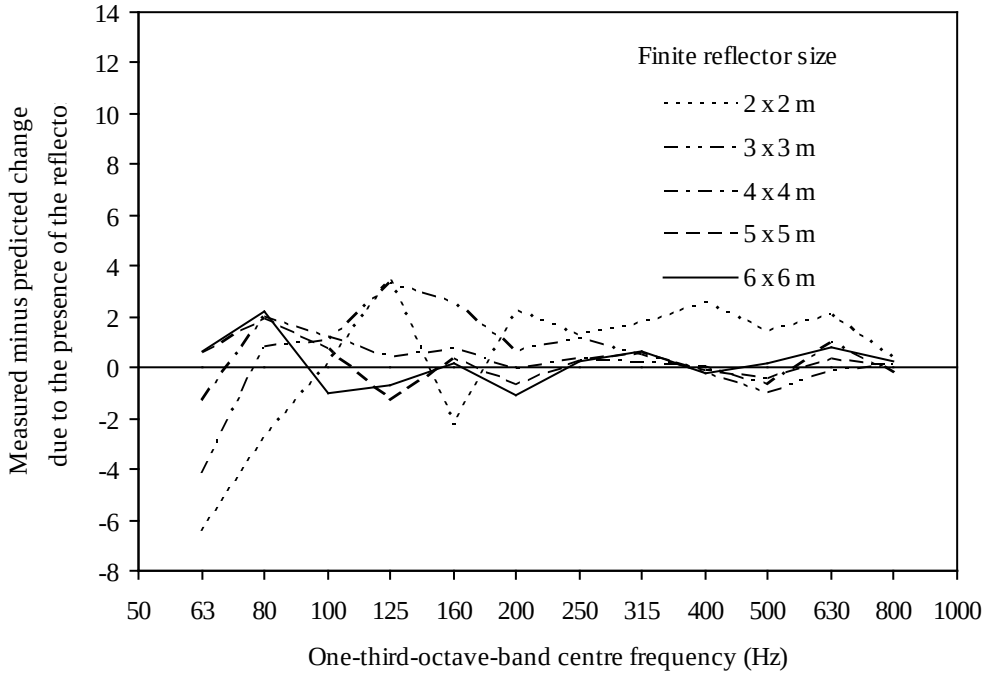

Fig. 9
Difference between the measured (finite reflector) and predicted (semi-infinite reflector) change in sound pressure level due to the presence of the reflector.

Note to typesetter: Excel has cut off the y-axis titles on both graphs. Please replace it with “Measured minus predicted change in SPL due to the presence of the reflector (dB)”

a)

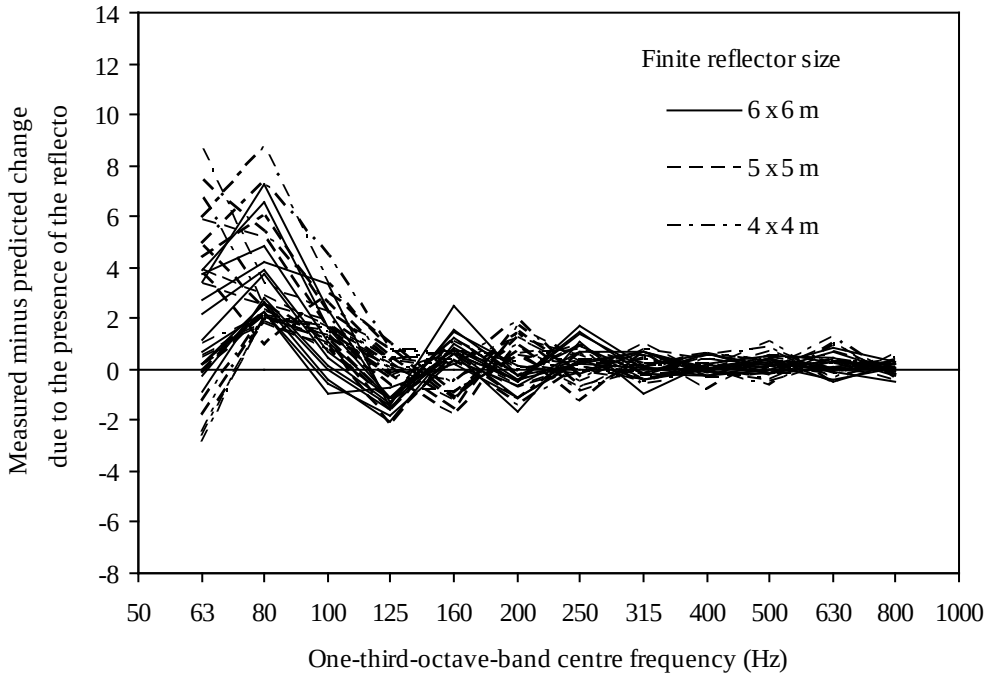
Finite reflector size
6 x 6 m
5 x 5 m
4 x 4 m
Measured minus predicted change due to the presence of the reflecto
14
12
10
8
6
4
2
0
-2
-4
-6
-8
50
63
80
100
125
160
200
250
315
400
500
630
800
1000
One-third-octave-band centre frequency (Hz)

b)

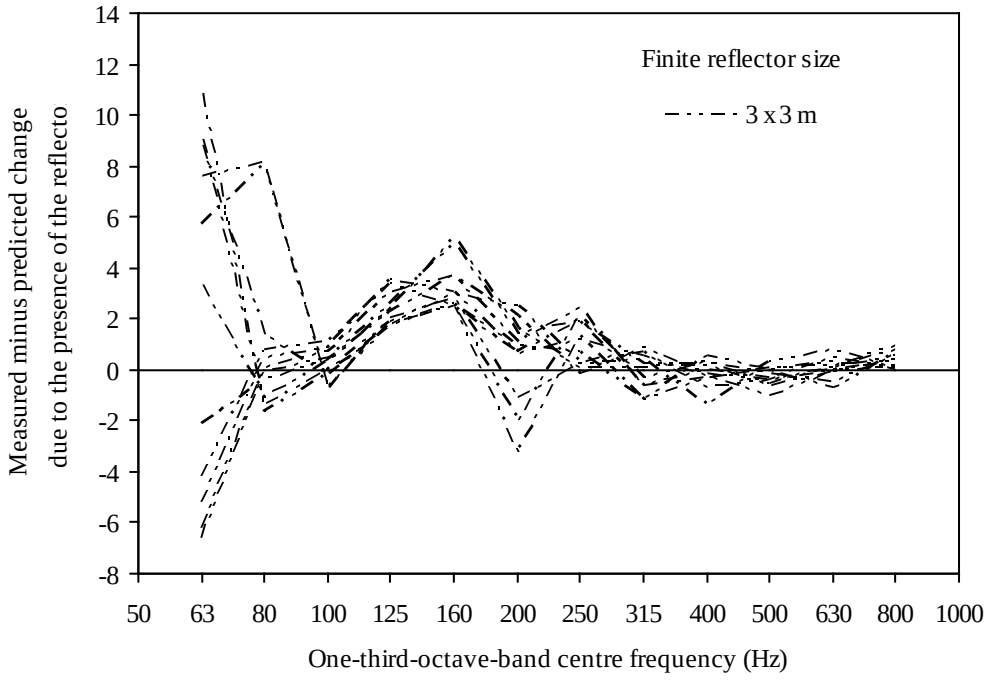
Finite reflector size
3 x 3 m
Measured minus predicted change due to the presence of the reflecto
14
12
10
8
6
4
2
0
-2
-4
-6
-8
50
63
80
100
125
160
200
250
315
400
500
630
800
1000
One-third-octave-band centre frequency (Hz)

c)

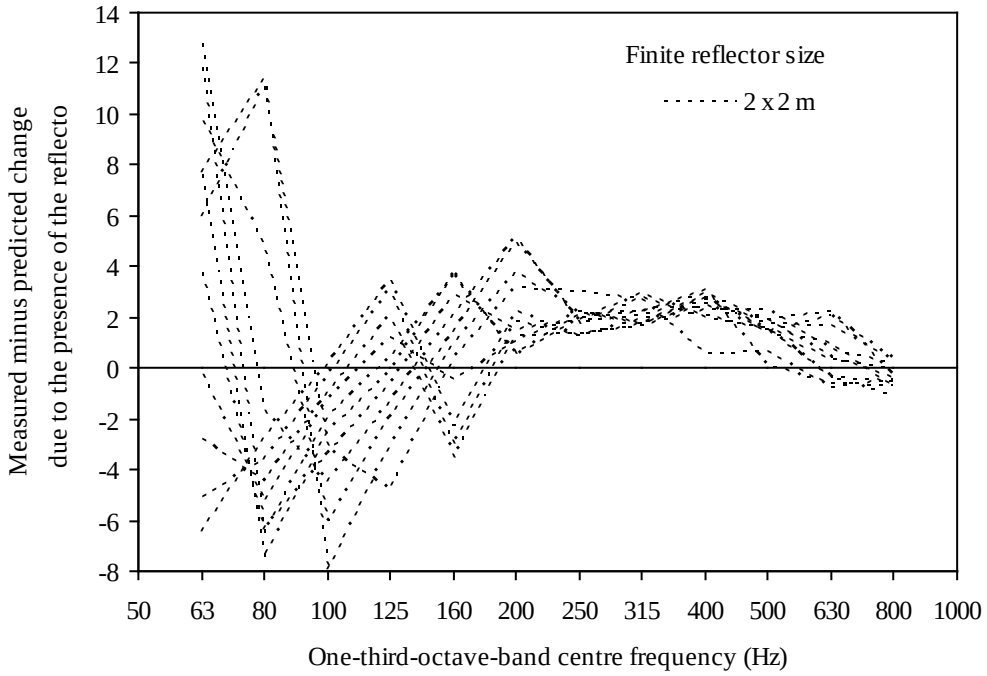

Fig. 10
Difference between the measured (finite reflector) and predicted (semi-infinite reflector) change in sound pressure level due to the presence of the reflector. For each size of reflector the 11 curves correspond to 0.1 m steps for the receiver-reflector distance, *d*, from 1 to 2 m inclusive.

Note to typesetter: Excel has cut off the y-axis titles on these three graphs. Please replace it with “Measured minus predicted change in SPL due to the presence of the reflector (dB)”